



1 Sequential Nutrient Uptake by Phytoplankton Maintains High Primary Productivity and  
2 Balanced Nutrient Stoichiometry

3

4

5 Kedong Yin<sup>1,2</sup> and Paul J. Harrison<sup>3</sup>

6

7

8 [1]{School of Marine Sciences, Sun Yat-sen University, Guangzhou, China}

9 [2]{Key Laboratory of Marine Resources and Coastal Engineering in Guangdong

10 Province, Guangzhou, China}

11 [3]{Department of Earth and Ocean Sciences, University of British Columbia, Vancouver

12 BC V6T 1Z4}

13 Correspondence to: Kedong Yin, School of Marine Science, Sun Yat-sen University (East

14 Campus), Guangzhou Higher Education Mega Center, Guangzhou, 510006, China.

15 Tel. +86 (0)20 3933 6536; Fax +86 (0)20 3933 6607. E-mail yinkd@mail.sysu.edu.cn

16

17

18

19 Running head: sequential nutrient uptake, nutritional strategy, nutrient stoichiometry

20

21

22

23

24



25     **Abstract**

26             We hypothesize that phytoplankton have the sequential nutrient uptake strategy in  
27     order to maintain nutrient stoichiometry and high primary productivity in the water column.  
28     Nutrient limited phytoplankton are capable of taking up the limiting nutrient first and they  
29     take up non-limiting nutrients when the limiting nutrient debt has been overcome. We used  
30     high resolution continuous vertical profiles of nutrients, nutrient ratios and on-board ship  
31     incubation experiments to test this hypothesis in the Strait of Georgia. At the surface in  
32     summer, ambient  $\text{NO}_3^-$  was depleted with excess  $\text{PO}_4^{3-}$  and  $\text{SiO}_4^{4-}$  remaining, and as a result,  
33     both N:P and N:Si ratios were low. The two ratios increased to about 10:1 and 0.45:1,  
34     respectively, at 20 m. Time series of vertical profiles showed that the leftover  $\text{PO}_4^{3-}$  continued  
35     to be removed, resulting in additional phosphorus storage by phytoplankton. There were  
36     various shapes of vertical profiles of N:P and at the nutricline it changed quickly in response  
37     to mixing events. A field incubation of seawater also demonstrated the sequential uptake of  
38      $\text{NO}_3^-$  (the most limiting nutrient) and then  $\text{PO}_4^{3-}$  and  $\text{SiO}_4^{4-}$  (the non-limiting nutrients). This  
39     sequential uptake strategy allows phytoplankton to acquire additional cellular phosphorus and  
40     silicon when they are available and wait for nitrogen to become available through frequent  
41     mixing of  $\text{NO}_3^-$  (or pulsed regenerated  $\text{NH}_4$ ). Thus, phytoplankton show variability of  
42     nutrient stoichiometry and are capable of maintaining high productivity by taking advantage  
43     of vigorous mixing regimes. To our knowledge, this is the first study to show the dynamics of  
44     continuous vertical profiles of N:P and N:Si ratios and to examine the responses of  
45     phytoplankton to nutrients supplied naturally by mixing events. The continuous nutrient  
46     profiles provided insight into the in situ dynamics of nutrient stoichiometry in the water  
47     column and the transient status of nutrient stoichiometry of phytoplankton in the field.

48

49



50 **1. Introduction**

51       The stoichiometry of the C:N:P Redfield ratio is an average across a wide range of  
52 species and environmental conditions and remains a central tenet in oceanography as it  
53 couples ecosystem processes with ocean biogeochemistry, which is driven by physical  
54 processes in oceans (Redfield, 1958). Four mechanisms have been proposed to explain the  
55 variability in C:N:P ratios in marine plankton, as summarized by Weber and Deutsch (2010).  
56 The first mechanism emphasizes the relationship between cellular elemental stoichiometry of  
57 phytoplankton and ambient nutrient ratios, i.e., the stoichiometry of the water column.  
58 Laboratory cultures of phytoplankton that are in the steady state usually display variable  
59 cellular N:P ratios with the nutrient N:P supply ratios. Based on the average Redfield ratio,  
60 this mechanism has been used to infer the most limiting nutrient for phytoplankton and to  
61 debate which nutrient, nitrogen or phosphorus, should be managed to control eutrophication  
62 effects (Conley et al., 2009). The second mechanism suggests that the elemental  
63 stoichiometry is taxonomy specific. Diatoms were reported to drawdown nutrients with a low  
64 nutrient C:P and N:P ratios (Geider and La Roche, 2002; Elser et al., 2003; Price, 2005),  
65 while marine cyanobacteria have higher C:P and N:P ratios (Karl et al., 2001; Bertilsson et  
66 al., 2003). Based on the resource allocation theory, the third mechanism proposed the  
67 “growth rate hypothesis”, which states that the elemental stoichiometry within a cell is  
68 controlled by the biochemical allocation of resources to different growth strategies  
69 (Falkowski, 2000; Elser et al., 2003; Klausmeier et al., 2004). Fast-growing cells may have a  
70 lower N:P ratio due to a larger allocation to P-rich assembly machinery of ribosomes  
71 (Loladze and Elser, 2011), whereas competitive equilibrium favors a greater allocation to P-  
72 poor resource acquisition machinery and therefore, higher N:P ratios. The fourth mechanism  
73 is related to the interference from dead plankton or organic detritus on the measurement of  
74 elemental composition of organic matter, which cannot be supported due to lack of such



75 measurements in oceans and coastal waters.

76 In culture experiments, sequential uptake of nutrients has been demonstrated for  
77 diatoms under N and Si limitation (Conway et al., 1976; Conway and Harrison, 1977;  
78 Harrison et al., 1989). Surge uptake of the limiting nutrient occurs when it is added to the  
79 culture, while the uptake of the non-limiting nutrient is slowed or stopped until the diatom  
80 has overcome its nutrient debt. Hence, the sequence of which nutrient is taken up first is  
81 directly related to the nutrient status of the phytoplankton. It is difficult to assess the  
82 nutritional status of phytoplankton in the field, but the application of laboratory results to the  
83 interpretation of vertical nutrient profiles can provide information on their nutritional status.  
84 To date, there have been no studies of sequential uptake of nutrients in the field using a series  
85 of high resolution vertical profiles of nutrients and their application to nutritional status of the  
86 phytoplankton.

87 In this study, we used high resolution continuous vertical profiles of N:P and N:Si  
88 ratios to examine how N:P and N:Si ratios respond to the mixing in a highly dynamic coastal  
89 water column and the uptake of nutrients. On-board ship incubation experiments were  
90 conducted to support the observations of changes in vertical profiles of N:P and N:Si ratios.  
91 We constructed seven conceptual profiles to illustrate how a vertical profile of N:P ratios  
92 changes with mixing and uptake of nitrogen and phosphorus and how they could indicate the  
93 nutritional status of the phytoplankton assemblage. The model also explains how N:P ratios  
94 respond to mixing, particularly at the nutriclines (nitracline for  $\text{NO}_3^-$ , phosphacline for  $\text{PO}_4^{3-}$   
95 and silicacline for  $\text{SiO}_4^{4-}$ ), and indicates which nutrient,  $\text{NO}_3^-$  or  $\text{PO}_4^{3-}$ , is taken up first in the  
96 water column. To our knowledge, this is the first study to show the dynamics of continuous  
97 vertical profiles of N:P and N:Si ratios and to examine the nutritional status of phytoplankton  
98 and their response to the supply of nutrients from water column mixing. We believe that our  
99 approach can add a new dimension to examining the in situ dynamics of nutrients in the water



column and illustrate the ecological role of phytoplankton stoichiometry in phytoplankton completion for nutrients.

102

### 103 **1.1. Conceptual Model of Variability in Vertical N:P ratios (Fig. 1)**

104

105 The Strait of Georgia (hereafter the Strait) is an inland sea that lies between Vancouver

106 Island and the mainland of British Columbia. It is an ideal area for studying the interactions

107 between mixing, nutrient vertical profiles and phytoplankton nutrient uptake because of its

108 relatively high biomass, frequent wind mixing and shallow (15 m) photic zone. The Strait is

109 biologically productive, but inorganic nitrogen is often undetectable in productive seasons in

110 the surface layer. The nutricline sitting within the euphotic zone is often associated with the

111 pycnocline. In the Strait, the ambient N:P ratio is ~10:1, similar to other coastal areas (Hecky

112 and Kilham, 1988).

113 We selected seven (T0 to T6) conceptual vertical profiles that we encountered in our

114 field studies and suggest events that likely occurred to produce these nutrient profiles (Fig. 1).

115 **T0:** In winter or after a strong wind event, the water column is homogeneously mixed,

116 and  $\text{NO}_3^-$  and  $\text{PO}_4^{3-}$  are uniformly distributed in the water column. **T1:** With the onset of

117 stratification,  $\text{NO}_3^-$  and  $\text{PO}_4^{3-}$  are taken up within the mixed layer. Assuming that the average

118 nutrient uptake ratio is N16:1P, a N:P uptake ratio that is >10:1 would decrease the ambient

119 N:P ratio to <10:1. **T2:** The uptake of  $\text{NO}_3^-$  and  $\text{PO}_4^{3-}$  proceeds at a N:P ratio >10:1 until  $\text{NO}_3^-$

120 is just depleted. At this time the N:P ratio is near 0 and some phosphate remains in the water

121 column. **T3:** The remaining phosphate is completely taken up and stored as extra/surplus

122 intracellular phosphate. **T4:** After cross-pycnocline mixing occurs, the ambient N:P ratio in

123 the newly mixed water should be the same as the ratio in the deep water. As a result, the

124 vertical profile of the N:P ratio will form a right angle on the top part of the nutricline. **T5:**

125 Depending on how long the phytoplankton are nutrient limited, their response to the mixed



126 limiting nutrient can be different. When N deficient phytoplankton take up N only, the curve  
 127 of the N:P ratio parallels the  $\text{NO}_3^-$  distribution curve and  $\text{PO}_4^{3-}$  is left behind in the water  
 128 column. **T6:** On the other hand, if phytoplankton take up  $\text{PO}_4^{3-}$  before  $\text{NO}_3^-$  (e.g. if  
 129 phytoplankton were severely N starved, and there is a lag in  $\text{NO}_3^-$  uptake), the N:P ratio  
 130 would be higher at the nutricline than below.

131 Similarly, this conceptual model can be applied to N,  $\text{SiO}_4^{4-}$  and N:Si ratios. The  
 132 ambient (N:Si) ratio is about 0.5:1 at 20 m in the Strait, with 20  $\mu\text{M}$   $\text{NO}_3^-$  and 40  $\mu\text{M}$   $\text{SiO}_4^{4-}$ .  
 133 As the average uptake ratio of N:Si is about 0.7-1:1 (equivalent to Si:N = 1.5-1:1)  
 134 (Brzezinski, 1985), the N:Si ratio decreases with depth.  $\text{SiO}_4^{4-}$  is rarely depleted and  
 135 therefore, the N:Si ratio is mainly determined by the distribution of  $\text{NO}_3^-$ . The continuous  
 136 uptake of  $\text{SiO}_4^{4-}$  without the uptake of  $\text{NO}_3^-$  can be inferred based on the comparison between  
 137 the gradient of N:Si and the silicacline. For example, a sharper gradient of the N:Si ratio than  
 138 the silicacline would indicate the continuous uptake of  $\text{SiO}_4^{4-}$  without the uptake of  $\text{NO}_3^-$  as in  
 139 T5 (Fig. 1)

## 140 **2. Materials and Methods**

### 141 **2.1. Station Locations**

142 The transect started from station S2, 8 km beyond the Fraser River mouth and under  
 143 the influence of the river plume and extended 108 km NW to S1 (well beyond the plume) in  
 144 the Strait of Georgia (Fig. 2). The station numbers are consistent with previous studies (Yin et  
 145 al., 1997a, b and c).

### 146 **2.2. Sampling and Data Processing**

147 The sampling was designed to investigate the distribution of nutrients ( $\text{NO}_3^-$ ,  $\text{PO}_4^{3-}$   
 148 and  $\text{SiO}_4^{4-}$ ) and N:P and N:Si ratios associated with mixing processes during August 6-14,  
 149 1991. Data at either an anchored station for 24 h, or a transect of a few stations within 10 h  
 150 was used. At each station, a vertical profile (0-25 m) of temperature, salinity, *in vivo*



151 fluorescence and selected nutrients (nitrate+nitrite, phosphate, silicate) were obtained. Only  
152 vertical profiles of nutrients are presented in this study. Other data (salinity, temperature and  
153 fluorescence) are published elsewhere (Yin et al., 1997a). The vertical profiling system has  
154 been described in detail by Jones et al. (1991) and Yin et al. (1995a). Basically, a hose  
155 connected to a water pump on deck was attached to the CTD probe or S4 (InterOcean®)  
156 which has the dual function of a CTD probe and a current meter. Seawater from the pump  
157 was connected into the sampling tubing of an AutoAnalyzer® on board ship for *in situ*  
158 nutrient measurements, while the CTD probe was lowered slowly into the water at 1 m min<sup>-1</sup>.  
159 Each sampling produced a high resolution continuous vertical profile of physical and  
160 biological parameters and thus the relationship between these parameters in the water column  
161 can be easily recognized. Data from a vertical profile (a datum point every 3 s) were  
162 smoothed over 15 s intervals. This smoothing reduced the fluctuations caused by ship's  
163 motion.

### 164 **2.3. Analysis of Nutrients**

165 All nutrients were determined using a Technicon AutoAnalyzer II. Salinity effects on  
166 nutrient analyses were tested on board ship and were found to be small. Therefore, no  
167 correction was made for salinity effects. Nitrate (plus nitrite) and phosphate were determined  
168 following the procedures of Wood et al. (1967) and Hager et al. (1968), respectively. The  
169 analysis of silicate was based on Armstrong et al. (1967).

### 170 **2.4. Field Incubation Experiments**

171 Niskin bottles (5 L) were used to take seawater samples and the samples were  
172 transferred to acid cleaned carboys (10 L). Subsamples of seawater were transferred to  
173 transparent polycarbonate flasks (1 L) and placed in Plexiglas tanks. The tanks were kept at  
174 the same temperature as the surface water by pumping seawater (from the ship's intake at 3  
175 m) through the tank. The incubation flasks were wrapped with 1 or 4 layers of neutral density



176 screening which corresponded to the light intensity from which the samples were taken (1 or  
 177 16 m). In the nutrient enrichment experiments,  $\text{NO}_3^-$ ,  $\text{PO}_4^{3-}$  and  $\text{SiO}_4^-$  were added to the  
 178 samples, yielding final concentrations of 20-30, 2-3 and 20-30  $\mu\text{M}$ , respectively. The  
 179 incubations lasted for 24 to 96 h, and samples were taken every 3-6 h for nutrients.

### 180 **3. Results**

181

#### 182 **3.1. Vertical Profiles of Nutrients and Nutrient Ratios**

183 At S3 near the edge of the Fraser River plume, the profiles documented changes  
 184 before (T1) and after wind mixing (T7). At T1, both  $\text{NO}_3^-$  and  $\text{PO}_4^{3-}$  were low in the surface  
 185 layer and N:P ratios were low ( $<2:1$ ) and increased to  $\sim 8:1$  at 20 m (Fig. 3). At T7, higher N:P  
 186 ratios of 16-20:1 occurred due to an increase in  $\text{NO}_3^-$  in the deep water.  $\text{SiO}_4^{4-}$  was  $\sim 30 \mu\text{M}$  at  
 187 the surface due to input from the Fraser River, and increased to 37  $\mu\text{M}$  at 20 m (Fig. 3). The  
 188 N:P ratio curve nearly formed a right angle at the top of the nutriclines when the gradient of  
 189 the nitracline was larger than that of the phosphacline. At T1, the N:Si ratio was near 0  
 190 because  $\text{NO}_3^-$  was near the detection limit, but started to increase along the nitracline at the  
 191 depth of the  $\text{SiO}_4^-$  minimum. At T7, N:Si increased more rapidly with the nitracline.

192 A strong wind event occurred on August 7 and the water column was mixed (Yin et  
 193 al., 1997a). We followed the change in the nutrient profiles and nutrient ratios from S3 near  
 194 the Fraser River plume, to P4 and P6 and the well beyond the plume to S1. At S3, N:P ratios  
 195 in the water column were  $>7:1$  when both  $\text{NO}_3^-$  and  $\text{PO}_4^{3-}$  were high after wind mixing, with  
 196 N:Si ratios being  $<0.5:1$  (Fig. 4). As the post-wind bloom of phytoplankton developed along  
 197 P4-P6 due to the newly supplied nutrients (Yin et al., 1997a), N:P ratio followed the  
 198 distribution of  $\text{NO}_3^-$  at P4, and decreased to 0 as  $\text{NO}_3^-$  was depleted at the surface at P6 (Fig.  
 199 4). It was clear that little  $\text{PO}_4^{3-}$  was consumed while  $\text{NO}_3^-$  was taken up. At the same time, the  
 200 silicacline deepened and paralleled the nitracline. At S1, N:P and N:Si ratios formed almost a  
 201 vertical line. N:P and N:Si ratios were  $\sim 8:1$  and  $0.5:1$ , respectively, in the deep water (Fig. 4).





202 The time series (T1, T3, T8 and T11) of Aug 8-9 captured changes over 1 or 2 days  
 203 after the wind mixing event at S1 that was well beyond the river plume (Fig. 5). At T1, N:P  
 204 and N:Si ratios were ~9:1 and 0.45:1 respectively with  $\text{NO}_3^-$  and  $\text{PO}_4^{3-}$  being 15 and 1.7  $\mu\text{M}$ ,  
 205 respectively, at the surface. At T3, N:P ratio remained constant at ~9:1, while concentrations  
 206 of  $\text{NO}_3^-$  and  $\text{PO}_4^{3-}$  decreased by 10 and 1  $\mu\text{M}$ , respectively, indicating an uptake N:P ratio of  
 207 10:1. In comparison, N:Si ratio decreased from T1 to T3 when  $\text{SiO}_4^{2-}$  decreased by 10  $\mu\text{M}$ ,  
 208 producing an uptake N:Si ratio of ~1:1. At T8, N:P ratio followed the  $\text{NO}_3^-$  distribution as  
 209  $\text{NO}_3^-$  decreased to ~0  $\mu\text{M}$  at the surface while  $\text{PO}_4^{3-}$  was still ~0.5  $\mu\text{M}$ . This indicated that  
 210  $\text{NO}_3^-$  uptake was more rapid than  $\text{PO}_4^{3-}$  uptake and hence  $\text{NO}_3^-$  mainly determined the  
 211 ambient N:P ratios. The N:Si uptake ratio of ~1:1 continued until T8. However, at T11, the  
 212 N:P ratio spiked higher in the top 5-10 m of the nutricline, suggesting a more rapid uptake of  
 213  $\text{PO}_4^{3-}$  relative to  $\text{NO}_3^-$  in the upper portion of the phosphacline (Fig. 5).

214 Changes in the profiles after the wind event on Aug 7 were followed over 5 days (Aug  
 215 10 – 14) at P5 that was still within the influence of the river plume as evidenced by the higher  
 216 surface  $\text{SiO}_4^{4-}$  at the surface (Fig. 6). On Aug 10-11, N:P ratios were higher at the surface  
 217 where the post-wind induced bloom occurred two days earlier, suggesting that uptake of  
 218  $\text{PO}_4^{3-}$  had caught up with uptake of  $\text{NO}_3^-$ . The right angle shape of the N:P ratio on Aug 12  
 219 occurred as the nutriclines became sharper due to entrainment of nutrients. By Aug 13, more  
 220  $\text{NO}_3^-$  was taken up at depth and the N:P ratio followed the deepening of the nitracline and  
 221  $\text{PO}_4^{3-}$  was left behind. On Aug 14,  $\text{PO}_4^{3-}$  started to decrease. During Aug 10-14, a minimum  
 222 in  $\text{SiO}_4^{4-}$  was present at an intermediate depth (5-10 m), coinciding with the top of the  
 223 nitracline, and the silicacline followed the nitracline below 10 m.

### 224 3.2. Changes in Nutrient Ratios During Field Incubations

225 On deck incubation experiments were used to examine changes in uptake ratios by  
 226 eliminating any effects due to mixing. Ambient N:P and N:Si ratios were lower at the surface



than at depth, indicating higher uptake of  $\text{NO}_3^-$  at the surface. The indication of a higher uptake ratio of N:P and N:Si was supported by field incubation experiments. During nutrient addition ( $\text{NO}_3^-$ ,  $\text{PO}_4^{3-}$  and  $\text{SiO}_4^{4-}$ ) bioassays on a sample from 1 m at P3, all nutrients decreased as fluorescence increased (Fig. 7). Ambient N:P and N:Si ratios decreased to almost 0:0 after 96 h, indicating more rapid uptake of  $\text{NO}_3^-$  than uptake of  $\text{PO}_4^{3-}$  and  $\text{SiO}_4^{4-}$ . The temporal decline in the N:P and N:Si ratios resembled the temporal progression during a bloom as illustrated in T0-T3 of the conceptual profiles (Fig. 1) and in the water column (S3, P4, P6) on August 8 (Fig. 4) and during the time series at S1 (Fig. 5). During the incubation, both  $\text{PO}_4^{3-}$  and  $\text{SiO}_4^{4-}$  continued to be drawn down after  $\text{NO}_3^-$  became undetectable (Fig. 7). In an earlier incubation experiment at S3 near the end of the phytoplankton bloom on June 8,  $\text{PO}_4^{3-}$  was depleted at 1 m, and both  $\text{NO}_3^-$  and  $\text{SiO}_4^{4-}$  continued to disappear with 2  $\mu\text{M}$   $\text{NO}_3^-$  and 4  $\mu\text{M}$   $\text{SiO}_4^{4-}$  being taken up. However, for the sample taken at 16 m,  $\text{PO}_4^{3-}$  (~0.5  $\mu\text{M}$ ) and  $\text{SiO}_4^{4-}$  (~5  $\mu\text{M}$ ) continued to disappear after 1.25  $\mu\text{M}$   $\text{NO}_3^-$  was depleted after 8 h (Fig. 8).

The water sample at S1 on June 4 was incubated for 30 h without an addition of nutrients (Fig. 9A). The initially low  $\text{NO}_3^-$  and  $\text{PO}_4^{3-}$  remained near depletion levels during the incubation, but  $\text{SiO}_4^{4-}$  decreased from 9 to <1  $\mu\text{M}$  (Fig. 9A), which indicated that an additional 8  $\mu\text{M}$   $\text{SiO}_4^{4-}$  was taken up in excess in relation to N and P. At the end of 30 h, nutrients were added (Fig. 9B). Both  $\text{NO}_3^-$  and  $\text{PO}_4^{3-}$  rapidly disappeared during the first 6 h, while  $\text{SiO}_4^{4-}$  decreased little (Fig. 9B), indicating a sequential uptake of  $\text{NO}_3^-$  and  $\text{PO}_4^{3-}$  since 8  $\mu\text{M}$   $\text{SiO}_4^{4-}$  was previously taken up as shown in Fig. 9A. The N:P ratio decreased faster after a single addition of  $\text{NO}_3^-$  or  $\text{PO}_4^{3-}$  alone than with additions of  $\text{NO}_3^-$  and  $\text{PO}_4^{3-}$  together (Fig. 9C), suggesting an interaction between the uptake of  $\text{NO}_3^-$  and  $\text{PO}_4^{3-}$ . The accumulative uptake ratio of  $\text{NO}_3^-$  to  $\text{PO}_4^{3-}$  increased with time, especially when only a single nutrient was present. The ratio of N:Si decreased with time, and the accumulative uptake ratio of N:Si exceeded 3:1 in the presence of  $\text{PO}_4^{3-}$  (Fig. 9C).



## 252 **4. Discussion**

253  
 254 The Strait is highly productive due to pulsed nutrient supplies and multiple  
 255 phytoplankton blooms in the shallow photic zone interacting with wind events, and  
 256 fluctuations in river discharge (Yin et al., 1997a; Yin et al., 1995c). Our results revealed  
 257 sequential nutrient uptake to optimize nutrient uptake efficiency and generate high primary  
 258 productivity by phytoplankton by taking advantage of pulsed nutrients in this highly dynamic  
 259 relatively shallow photic zone.

### 260 **4.1. Responses of N:P and N:Si ratios to vertical mixing and uptake of nutrients**

261 A vertical profile of N:P and N:Si ratios represents a snapshot of the mixing and the  
 262 uptake of N, P and Si by phytoplankton in the water column. The depletion zone of the most  
 263 limiting nutrient in the euphotic zone ends at a depth where the uptake of nutrients just  
 264 balances the upward flux of nutrients through the nutricline, as indicated in T3 in the  
 265 conceptual profiles (Fig. 1). Different responses of nutrient uptake to pulsed nutrients by  
 266 mixing, appear to depend on the previous stability of the water column, the depth of the  
 267 euphotic zone and nutritional status of phytoplankton. Our observations spanned all seven  
 268 conceptual profiles (Fig. 1) and indicated the dynamic processes influencing the sequence of  
 269 nutrient uptake that is determined by the nutritional status of the phytoplankton. The change  
 270 in the profiles of the N:P ratio from S3 to P6 (Fig. 4) displayed the spring bloom-like  
 271 progression as illustrated in conceptual profiles of T0-T3 (Fig. 1) after the wind mixing event.  
 272 Various responses of the N:P ratios were similar to the conceptual profiles T4, T5 and T6  
 273 (Fig. 1). There was a right angle pattern in the N:P ratio sitting on the top of the nutriclines at  
 274 ~7 m in T7 of Fig. 3 and also at 6 m at P5 (Aug 12, Fig. 6) that was similar to the conceptual  
 275 profile in T4 (Fig. 1). There were parallel lines between the nitracline and the N:P ratio curve  
 276 on Aug 12, Fig. 6) that was similar to the conceptual profile in T5 (Fig. 1). At S1, there was a  
 277 spike in the N:P ratio curve at T11 (Fig. 5) at the top of the nutricline due to continued uptake



278 of  $\text{PO}_4^{3-}$  with  $\text{NO}_3^-$  being depleted during the time period from T1 to T8 (Fig. 5), as illustrated  
 279 in the conceptual profile T6 (Fig. 1). The spike in the N:P ratio was continuously observed on  
 280 Aug 10 at P5 (Fig. 6).

281

#### 282 **4.2. Sequential Nutrient Uptake for Balanced Stoichiometry and Nutritional** 283 **Optimization**

284 Phytoplankton can take advantage of the dynamic mixing regimes and optimize their  
 285 growth rates by taking up nutrients sequentially. The disappearance of nutrients during the  
 286 incubation resembled the temporal progression of a bloom as illustrated in T0-T3 of the  
 287 conceptual profiles (Fig. 1) and in the water column (S3, P4, P6; Fig. 4), or during the time  
 288 series at S1 (Fig. 5).

289 Nutrient deficiency results in a decrease in the cellular content of the limiting nutrient  
 290 and an increase in the cellular content of other non-limiting nutrients. Earlier studies found  
 291 that N limitation results in excess cellular content of P and Si (Conway and Harrison, 1977;  
 292 Healey, 1985; Berdalet et al., 1996). Some phytoplankton develop enhanced uptake of the  
 293 limiting nutrient such as  $\text{NH}_4$  and  $\text{PO}_4^{3-}$  upon its addition after a period of nutrient limitation  
 294 or starvation and there is an accompanying shut down of the non-limiting nutrient (Conway et  
 295 al., 1976; Conway and Harrison, 1977; McCarthy and Goldman, 1979). A few hours of  
 296 enhanced N uptake quickly overcomes the N debt since the enhanced uptake rate is many  
 297 times faster than the growth rate (Conway et al., 1976). For example, enhanced uptake of  
 298 phosphorus could double internal P within 5 min to 4 h depending on the degree of P  
 299 limitation and the pulsed concentration of  $\text{PO}_4^{3-}$  (Healey, 1973). After the nutrient debt has  
 300 been overcome by enhanced uptake, the uptake of non-limiting nutrients returns to normal  
 301 after the cell quota of the limiting nutrient is maximal (Collos, 1986). The sequential uptake  
 302 of a limiting nutrient and then the uptake of both the non-limiting and limiting nutrient is



303 advantageous to allow phytoplankton to maintain maximum growth rates over several cell  
304 generations.

### 305 **4.3. Significance of Sequential Uptake of Nutrients**

306       There are two essential strategies used by phytoplankton to cope with a pulse of the  
307 limiting nutrient (Collos, 1986). One strategy is the ‘growth’ response where phytoplankton  
308 uptake of the limiting nutrient and cellular growth are coupled. The other strategy is the  
309 “storage” response where phytoplankton have the capability of accumulating large internal  
310 nutrient pools, resulting in extensive uncoupling between uptake and growth, and a lag in cell  
311 division of up to 24 h following a single addition of the limiting nutrient. The former strategy  
312 would have the competitive advantage under frequent pulses of the limiting nutrient, whereas  
313 the latter strategy presents an ecological advantage when the nutrient pulsing frequency is  
314 lower than cell division rate. In the Strait, the chlorophyll maximum was frequently observed  
315 at the nutricline (Cochlan et al., 1990; Yin et al., 1997 a, b and c). At Stn S2, there was the  
316 chlorophyll maximum at 7 m during August 7 which contained 4 times more phytoplankton  
317 cells than at the surface. The phytoplankton community in the chlorophyll maximum  
318 contained diatoms such as *Chaetoceros* and *Thalassiosira* which use the ‘growth’ and  
319 ‘storage’ strategies respectively. In either case, the previous storage of non-limiting nutrients  
320 would allow phytoplankton to utilize the limiting nutrient and thus maximize phytoplankton  
321 growth by saving the energy expenditure associated with taking up non-limiting nutrients  
322 under limiting irradiance. This may explain why there were various modes or patterns of the  
323 N:P ratio at the nutricline, which indicates the different strategies of taking up nutrients  
324 sequentially based on the nutritional status of phytoplankton. The sequential uptake strategy  
325 allows phytoplankton to use the “storage” capacity for non-limiting nutrients and the  
326 “growth” response for the most limiting nutrient when it becomes available by mixing  
327 processes.



Sequential uptake of nutrients by phytoplankton can be a fundamental mechanism in maintaining high productivity in the water column where there are frequent mixing events in coastal waters. The sequential uptake strategy largely occurs at the nutraclines near or at the bottom of the photic zone. There is a consistent association between the nutriclines and the chlorophyll maximum in various aquatic environments (Cullen, 2015) and it is also common in the Strait (Harrison et al., 1991). There is a frequent upward flux of nutrients through the nutricline due to entrainment in the Strait (Yin et al., 1995a, b and c) and by internal waves in the open ocean. Phytoplankton in the chlorophyll maximum are generally nutrient sufficient and when these cells are brought up to the surface during entrainment or wind mixing (Yin et al., 1995a), they can quickly photosynthesize (Yin et al., 1995c). When phytoplankton exhaust the most limiting nutrient, their internal nutrient pool decreases and they sink down to the nutriclines and take up the abundant nutrients there. Thus, the cycle of sequential uptake of limiting and then the non-limiting nutrients may reduce nutrient deficiency in phytoplankton.

Sequential uptake of nutrients can be an important process to maintain the phytoplankton nutrient stoichiometry. Carbon fixation continues after a nutrient becomes deficient (Elrifi and Turpin, 1985; Goldman and Dennett, 1985) and the storage of organic carbon of a higher POC:N ratio is common in phytoplankton (Healey, 1973). When phytoplankton cells with excessive organic carbon due to limitation of a nutrient, sink from the upper euphotic zone to the nutricline where light becomes limiting, uptake of other nutrients occurs by utilizing stored organic carbon, leading to an increase in the cellular N and P quotas. Thus, the ratios of carbon to other nutrients approach optimum stoichiometry. POC:N ratios at Stn S2 and S3 were observed to be between 6:1 and 7:1 in the water column, even though both ambient  $\text{NO}_3^-$  and  $\text{PO}_4^{3-}$  were near detection limits (Fig. 10). This demonstrates the lack of ambient nitrogen limitation on the cellular nutrient stoichiometry.



353 Even at Stn S1 where entrainment and mixing were not as strong as at Stns S2 and S3, the  
354 POC:N ratio was only slightly higher than 7:1 (Fig. 10).

## 355 **5. Conclusion**

356 As summarized in the introduction, there are four mechanisms to explain the variability in  
357 C:N:P ratios. The sequential uptake of nutrients offers another mechanism for explaining the  
358 variability in the nutrient stoichiometry in phytoplankton in the euphotic zone. The use of  
359 in-situ continuous vertical profiles in this showed that deficiency of a nutrient that is based  
360 on the ambient nutrient ratio could be transient and overcome by the sequential uptake during  
361 the nutrient mixing regimes. The sequential uptake of nutrients is an important strategy for  
362 phytoplankton to maintain high primary productivity and near optimum cellular nutrient  
363 stoichiometry.

## 364 **Authors contributions**

365 K. Yin collected data and wrote the manuscript.  
366 PJ Harrison supported the research cruise for collection of data and designed the sampling  
367 plan.

## 368 **Competing interests**

369 The authors declare that they have no conflict of interest.

## 370 **Acknowledgements**

371 We thank Dr. Mike St. John who coordinated the cruise. We acknowledge the Department of  
372 Fisheries and Oceans for providing ship time, and the officers and crew of C.S.S. Vector for  
373 their assistance. This research was funded by a Natural Sciences and Engineering Research  
374 Council of Canada (NSERC) Strategic grant awarded to Prof. Paul J. Harrison. K. Yin  
375 acknowledges the continuing support of NSFC 91328203 to this study.

376

377

378



## 379 References

- 380 Armstrong, F. A. J., Stearns, C. R., and Strickland, J. D. H.: The measurement of upwelling  
381 and subsequent biological processes by means of the Technicon Autoanalyzer® and  
382 associated equipment, Deep Sea Research and Oceanographic Abstracts, 14, 381-389,  
383 1967.
- 384 Berdalet, E., Marrasé, C., Estrada, M., Arin, L., and MacLean, M. L.: Microbial community  
385 responses to nitrogen- and phosphorus-deficient nutrient inputs: microplankton  
386 dynamics and biochemical characterization, J. Plank. Res., 18, 1627-1641, 1996.
- 387 Bertilsson, S., Berglund, O., Karl, D. M., and Chisholm, S. W.: Elemental composition of  
388 marine Prochlorococcus and Synechococcus: Implications for the ecological  
389 stoichiometry of the sea, Limnol. Oceanogr., 48, 1721-1731, 2003.
- 390 Brzezinski, M. A.: The Si:C:N ratio of marine diatoms: interspecific variability and the effect  
391 of some environmental variables, J. Phycol., 21, 247-257, 1985.
- 392 Cochlan, W. P., Harrison, P. J., Clifford, P. J., and Yin, K.: Observations on double  
393 chlorophyll maxima in the vicinity of the Fraser River plume, Strait of Georgia,  
394 British Columbia, J. Exp. Mar. Biol. Ecol., 143, 139-146, 1990.
- 395 Collos, Y.: Time-lag algal growth dynamics: biological constraints on primary production in  
396 aquatic environments, Mar. Ecol. Prog. Ser., 33, 193-206, 1986.
- 397 Conley, D. J., Paerl, H. W., Howarth, R. W., Boesch, D. F., Seitzinger, S. P., Havens, K. E.,  
398 Lancelot, C., and Likens, G. E.: Controlling eutrophication: nitrogen and phosphorus,  
399 Science, 323, 1014-1015, 2009.
- 400 Conway, H. L. and Harrison, P. J.: Marine diatoms grown in chemostats under silicate or  
401 ammonium limitation IV. Transient response of *Chaetoceros debilis*, *Skeletonema*  
402 *costatum* and *Thalassiosira gravida* to a single addition of the limiting nutrient, Mar.  
403 Biol., 43, 33-43, 1977.
- 404 Conway, H. L., Harrison, P. J., and Davis, C. O.: Marine diatoms grown in chemostats under  
405 silicate or ammonium limitation. II. Transient response of *Skeletonema costatum* to a  
406 single addition of the limiting nutrient, Mar. Biol., 35, 187-199, 1976.
- 407 Cullen, J.J.: Subsurface chlorophyll maximum layers: enduring enigma or mystery solved?,  
408 Annu. Rev. Mar. Sci., 7, 207-239, 2015.
- 409 Elrifi, I. R. and Turpin, D. H.: Steady-state luxury consumption and the concept of optimum  
410 nutrient ratios: a study with phosphate and nitrate limited *Selenastrum minutum*  
411 (Chlorophyte), J. Phycol., 21, 592-602, 1985.
- 412 Elser, J. K., Acharya, M., Kyle, J., Cotner, W., Makino, T., Markow, T., Watts, S., Hobbie, W.,  
413 Fagan, J., Schade, J., Hood, J., and Sterner, R. W.: Growth rate-stoichiometry  
414 couplings in diverse biota, Ecol. Lett., 6, 936-943, 2003.
- 415 Falkowski, P. G.: Rationalizing elemental ratios in unicellular algae, J. Phycol., 36, 3-6, 2000.





- 416 Geider, R.J. and La Roche, J.: Redfield revisited: variability of C:N:P in marine microalgae  
417 and its biochemical basis, *Eur. J. Phycol.*, 37, 1-17, 2002.
- 418 Goldman, J. C. and Dennett, M. R.: Photosynthetic responses of 15 phytoplankton species to  
419 ammonium pulsing, *Mar. Ecol. Prog. Ser.*, 20, 259-264, 1985.
- 420 Hager, S. W., Gordon, L. I., and Park, P. K.: A practical manual for the use of the Technicon  
421 AutoAnalyzer in seawater nutrient analysis, Final Rep. Bur. Commer. Fish., Contract,  
422 pp14-17, 1968.
- 423 Harrison, P. J., Parslow, J. S., and Conway, H. L.: Determination of nutrient uptake kinetics  
424 parameters: a comparison of methods, *Mar. Ecol. Prog. Ser.*, 52, 301-312, 1989.
- 425 Harrison, P. J., Clifford, P. J., Cochlan, W. P., Yin, K., St. John, M. A., Thompson, P. A.,  
426 Sibbald, M. J., and Albright, L. J.: Nutrient and plankton dynamics in the Fraser-river  
427 plume, Strait of Georgia, British-Columbia, *Mar. Ecol. Prog. Ser.*, 70, 291-304, 1991.
- 428 Healey, F. P.: Inorganic nutrient uptake and deficiency in algae, *CRC Crit. Rev. Microbiol.*, 3,  
429 69-113, 1973.
- 430 Healey, F. P.: Interacting effects of light and nutrient limitation on growth rate of  
431 *Synechococcus linearis* (Cyanophyceae), *J. Phycol.*, 21, 134-146, 1985.
- 432 Hecky, R. E. and Kilham, P.: Nutrient limitation of phytoplankton in freshwater and marine  
433 environments: a review of recent evidence on the effects of enrichment, *Limnol.*  
434 *Oceanogr.*, 33, 786-822, 1988.
- 435 Jones, D. M., P. J., Harrison, P. J., Clifford, P. J., Yin, K., and John, M. St.: A computer-based  
436 system for the acquisition and display of continuous vertical profiles of temperature,  
437 salinity, fluorescence and nutrients, *Water Res.*, 25, 1545-1548, 1991.
- 438 Karl, D. M., Björkman, K. M., Dore, J. E., Fujieki, L., Hebel, D. V., Houlihan, T., Letelier, R.  
439 M., and Tupas, L. M.: Ecological nitrogen-to-phosphorus stoichiometry at station  
440 aloha, *Deep Sea Res. PT II*, 48, 1529-1566, 2001.
- 441 Klausmeier, C. A., Litchman, E., Daufresne, T. and Levin, S. A.: Optimal nitrogen-to-  
442 phosphorus stoichiometry of phytoplankton, *Nature*, 429, 171-174, 2004.
- 443 Loladze, I. and Elser, J.: The origins of the Redfield nitrogen-to-phosphorus ratio are in a  
444 homeostatic protein-to-rRNA ratio, *Ecol. Lett.*, 14, 244-250, 2011.
- 445 McCarthy, J. J., and Goldman, J. C.: Nitrogenous nutrition of marine phytoplankton in  
446 nutrient depleted waters, *Science*, 203, 670-672, 1979.
- 447 Price, N. M.: The elemental stoichiometry and composition of an iron-limited diatom,  
448 *Limnol. Oceanogr.*, 50, 1159-1171, 2005.
- 449 Redfield, A. C.: The biological control of chemical factors in the environment, *Am. Sci.*, 46,  
450 205-222, 1958.
- 451 Wood, E. D., Armstrong, F. A. J., and Richards, F. A.: Determination of nitrate in sea water  
452 by cadmium-copper reduction to nitrite, *J. Mar. Biol. Ass. U.K.*, 47, 23-31, 1967.



- 453 Weber, T. S., and Deutsch, C.: Ocean nutrient ratios governed by plankton biogeography,  
454 Nature, 467, 550-554, 2010.
- 455 Yin, K., Harrison, P. J., Pond, S., and Beamish, R. J.: Entrainment of nitrate in the Fraser  
456 River plume and its biological implications. I. Effects of salt wedge, Estuar. Coast.  
457 Shelf Sci., 40, 505-528, 1995a.
- 458 Yin, K., Harrison, P. J., Pond, S., and Beamish, R. J.: Entrainment of nitrate in the Fraser  
459 River plume and its biological implications. II. Effects of spring vs neap tides and  
460 river discharge, Estuar. Coast. Shelf Sci., 40, 529-544, 1995b.
- 461 Yin, K., Harrison, P. J., Pond, S., and Beamish, R. J.: Entrainment of nitrate in the Fraser  
462 River plume and its biological implications. III. Effects of winds, Estuar. Coast. Shelf  
463 Sci., 40, 545-558, 1995c.
- 464 Yin, K., Goldblatt, R. H., Harrison, P. J., John, M. A. St., Clifford, P. J., and Beamish, R. J.:  
465 Importance of wind and river discharge in influencing nutrient dynamics and  
466 phytoplankton production in summer in the central Strait of Georgia, Mar. Ecol. Prog.  
467 Ser., 161, 173-183, 1997a.
- 468 Yin, K., Harrison, P. J., and Beamish, R. J.: Effects of a fluctuation in Fraser River discharge  
469 of primary production in the central Strait of Georgia, British Columbia, Canada, Can.  
470 J. Fish Aquat. Sci., 54, 1015-1024, 1997b.
- 471 Yin, K., Harrison, P. J., Goldblatt, R. H., John, M. A. St., and Beamish, R. J.: Factors  
472 controlling the timing of the spring bloom in the Strait of Georgia estuary, British  
473 Columbia, Canada, Can. J. Fish Aquat. Sci., 54, 1985-1995, 1997c.
- 474



## Figures captions

Figure 1. Conceptual vertical profiles of the dynamics of N, P and N:P ratios. T0 to T3 represent a time series nutrient uptake during bloom development and T4 to T6 indicate subsequent vertical mixing of nutrients and subsequent uptake. The short horizontal line near the middle of the depth axis indicates the euphotic zone depth. At T2, N disappears first and P is left which continues to be taken up at T3. T4 represents mixing of nutrients into the bottom of the photic zone and phytoplankton have not taken up these nutrients yet. At T5, N is taken up first before P, while at T6, P is taken up first before N.

Figure 2. Map of the Strait of Georgia showing the study area and the sampling stations.

Figure 3. Two vertical profiles (T1=12:15 and T7=06:15) in the time series for August 6-7, 1991 of nutrients at S3. Left panel:  $\text{NO}_3^-$ ,  $\text{PO}_4^{3-}$  and N:P ratios. Right panel:  $\text{SiO}_4^{4-}$  and N:Si.

Figure 4. Vertical profiles at S3 near the Fraser River plume to P4 and P6 finally to S1 that was well beyond the plume (108 km away) during August 8, 1991. Left panel:  $\text{NO}_3^-$ ,  $\text{PO}_4^{3-}$  and N:P ratios. Right panel:  $\text{SiO}_4^{4-}$  and N:Si ratios.

Figure 5. Selected vertical profiles at S1 during the time series (T1, T3, T8 and T11) of August 8-9, 1991. Left panel:  $\text{NO}_3^-$ ,  $\text{PO}_4^{3-}$  and N:P ratios. Right panel:  $\text{SiO}_4^{4-}$  and N:Si ratios.

Figure 6. Vertical profiles in the time series at P5 during August 10-14, 1991. Left panel:  $\text{NO}_3^-$ ,  $\text{PO}_4^{3-}$  and N:P ratios. Right panel:  $\text{SiO}_4^{4-}$  and N:Si ratios.

Figure 7. Time course of duplicate in vivo fluorescence,  $\text{NO}_3^-$ ,  $\text{PO}_4^{3-}$  and  $\text{SiO}_4^{4-}$ , and N:P and N:Si ratios during an in situ incubation of a water sample taken from



1 m at P3 on August 11 (11:45).  $\text{NO}_3^-$ ,  $\text{PO}_4^{3-}$  and  $\text{SiO}_4^{4-}$  were added to the water sample at  $T=0$  before the incubation.

Figure 8. Time course  $\text{NO}_3^-$ ,  $\text{PO}_4^{3-}$  and  $\text{SiO}_4^{4-}$  during the field incubation of water samples taken at Stn S3 during June 8, 1989. Top panel: sample taken at 1 m and the incubation was done under 1 layer of screening. Bottom panel: sample taken at 16 m and incubated under 4 layers of screening.

Figure 9. Time course of  $\text{NO}_3^-$ ,  $\text{PO}_4^{3-}$ , and  $\text{SiO}_4^{4-}$  during the field incubation of a water sample taken at Stn S1 on June 4, 1990. (A) No nutrients were added to the sample during the first 28 h; (B) nutrients were added in 8 treatments: no additions,  $\text{NO}_3^-$  alone (+N),  $\text{PO}_4^{3-}$  alone (P),  $\text{SiO}_4^{4-}$  alone (+Si),  $\text{NO}_3^-$  and  $\text{PO}_4^{3-}$  together (+N+P),  $\text{NO}_3^-$  and  $\text{SiO}_4^{4-}$  (+N+Si),  $\text{PO}_4^{3-}$  and  $\text{SiO}_4^{4-}$  (+P+Si) and all three (+N+P+Si); (C) Ambient and uptake nutrient ratios calculated from the time course in (B).

Figure 10. Vertical profiles of particulate organic C:N ratios at stations Stn S2, S3 and S1 along the increasing distance from the river during August 20-23, 1990.

Fig. 1

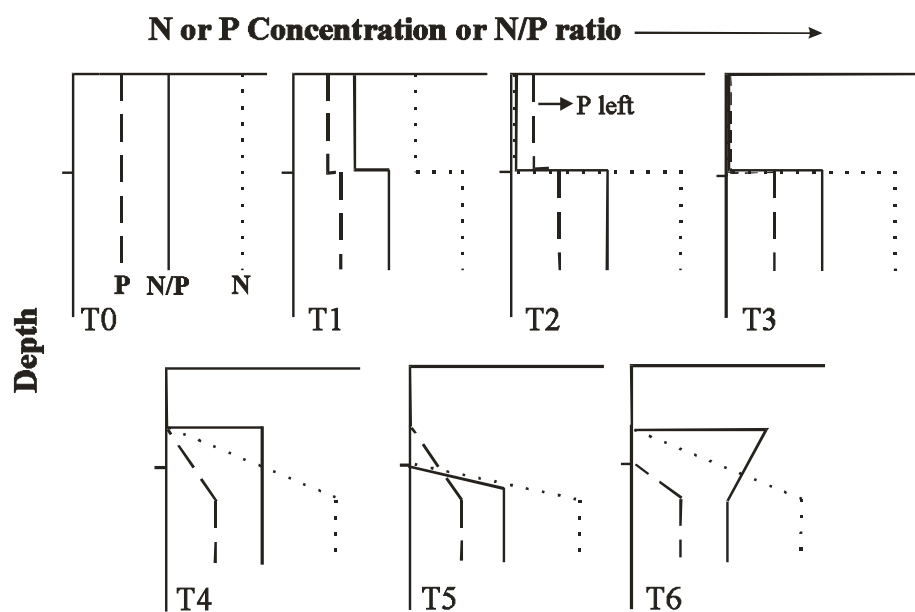


Fig. 2

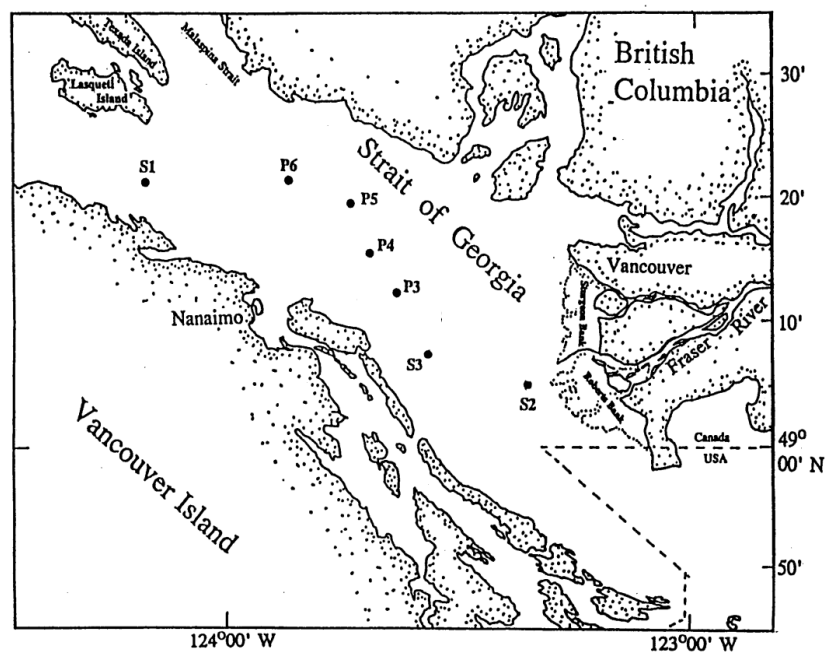


Fig. 3

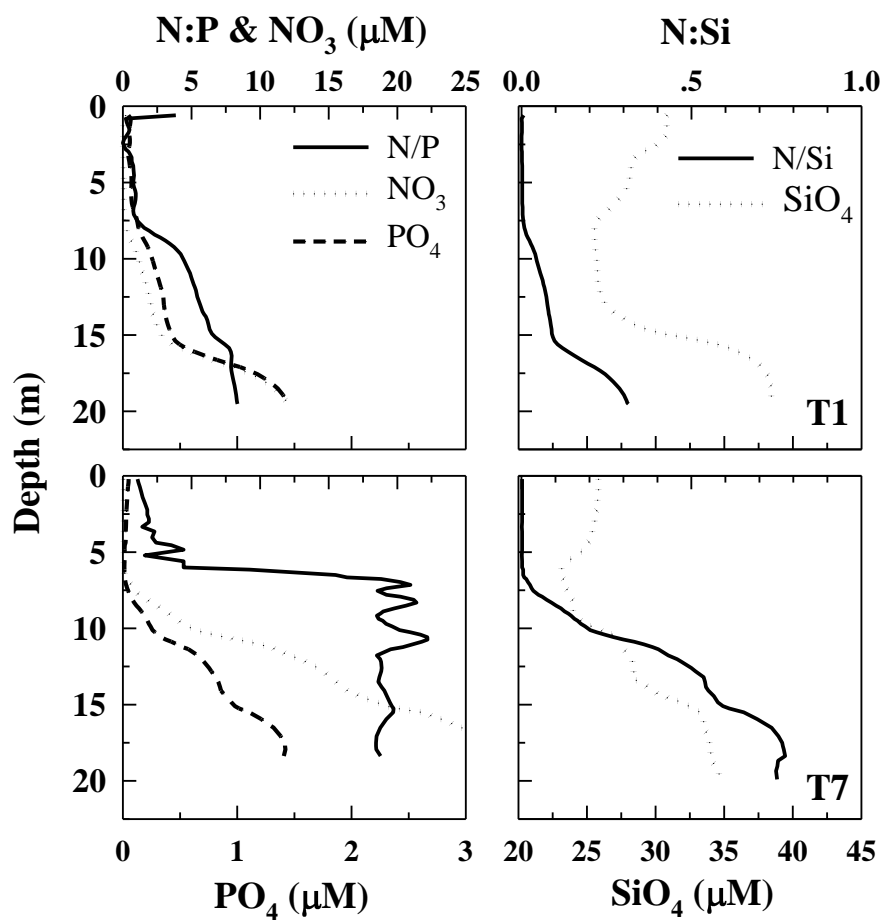


Fig. 4

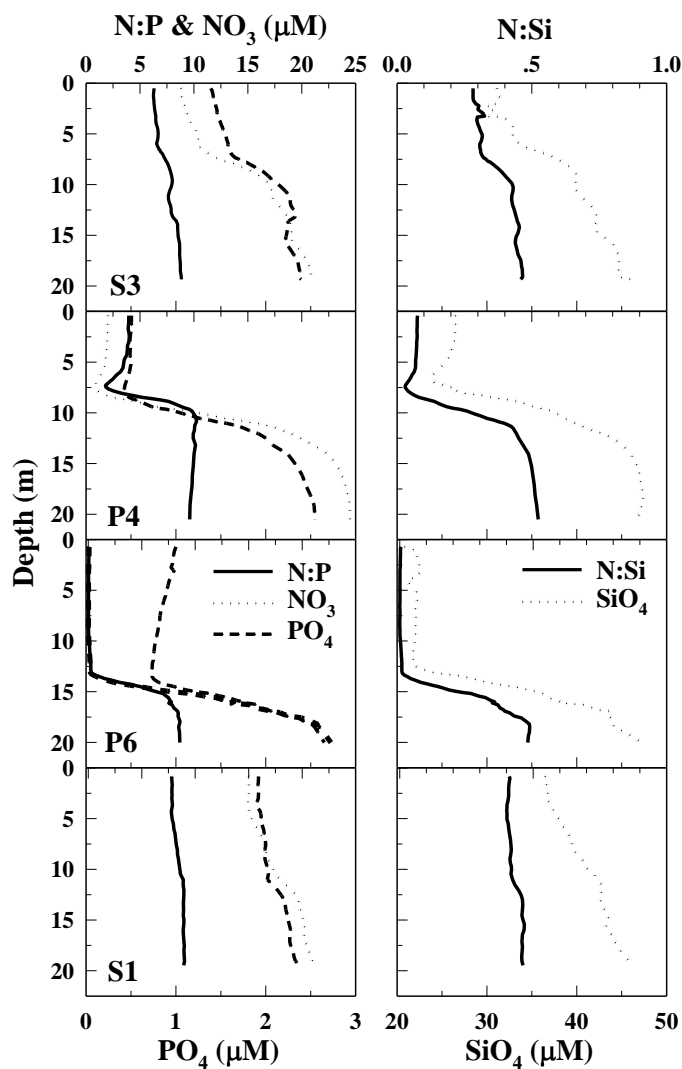




Fig. 5

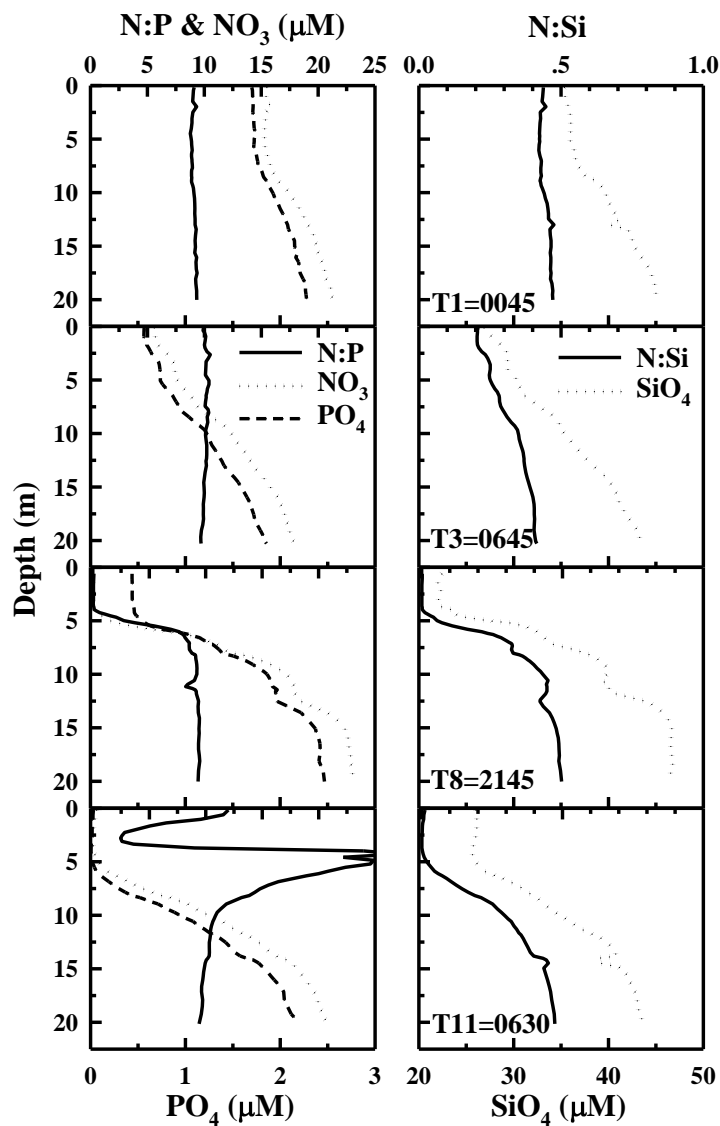


Fig. 6

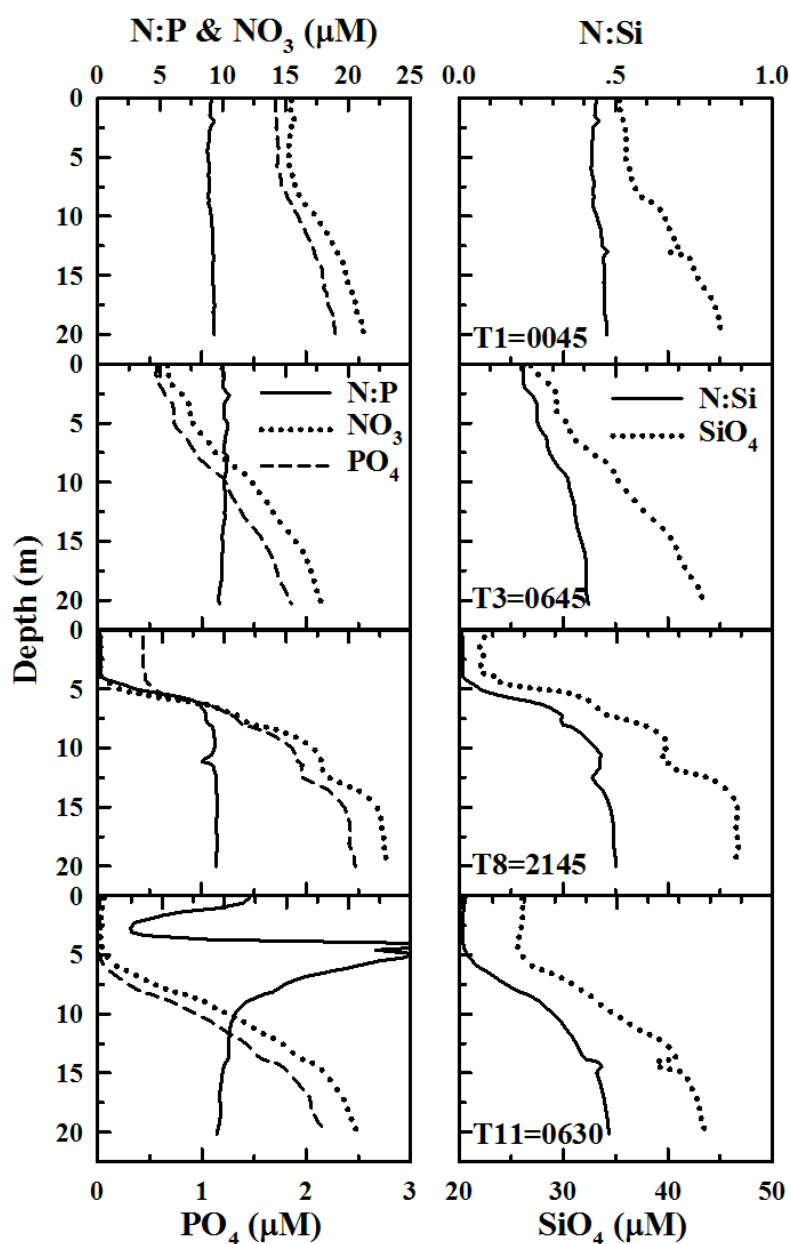


Fig. 7

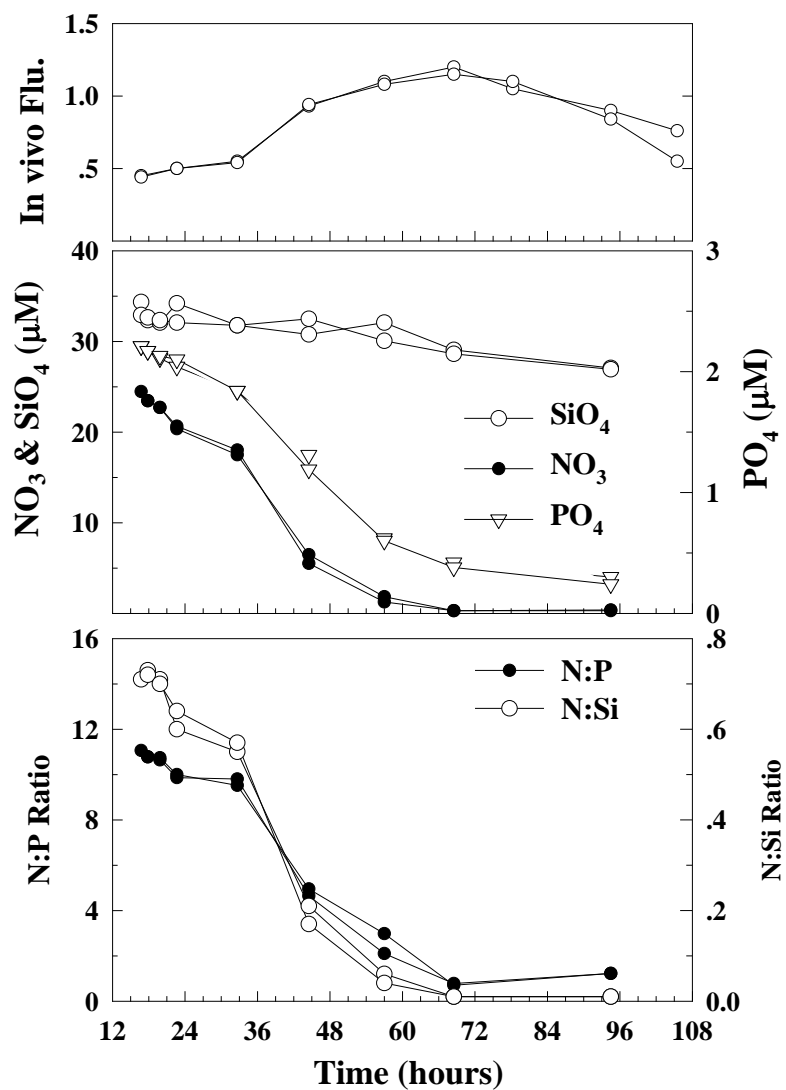


Fig. 8

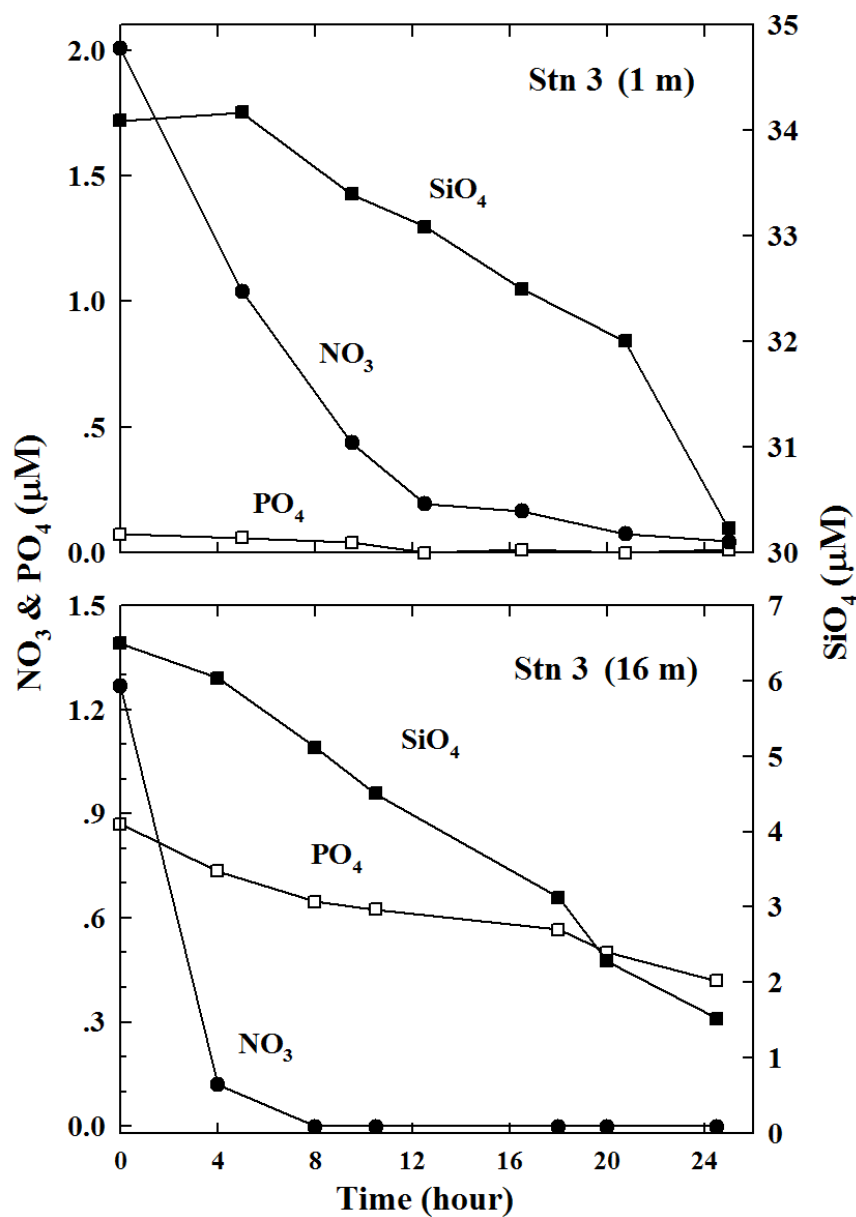


Fig. 9A

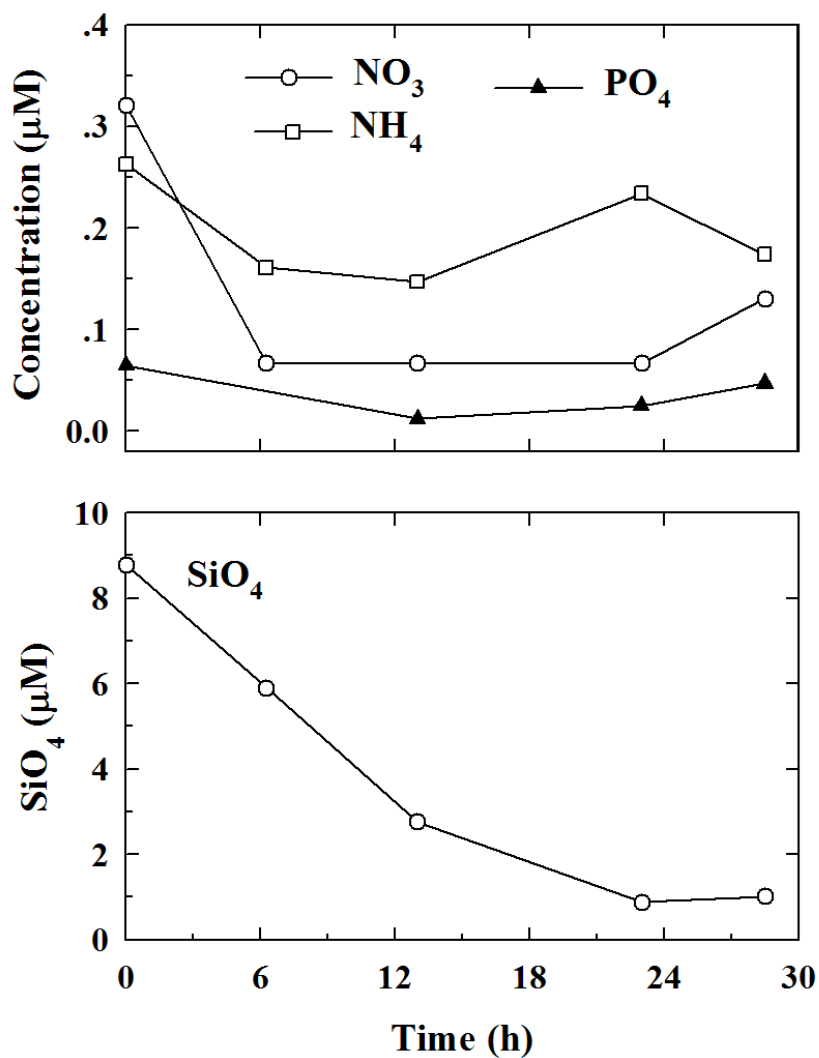


Fig. 9B

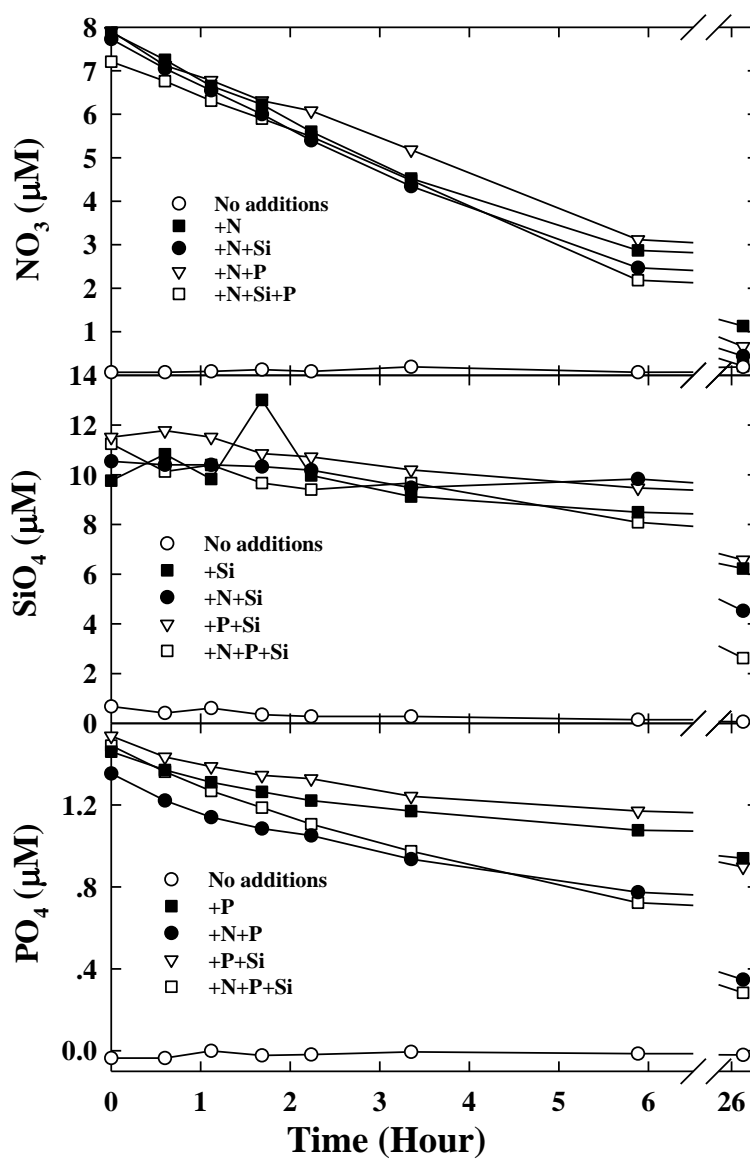


Fig. 9C

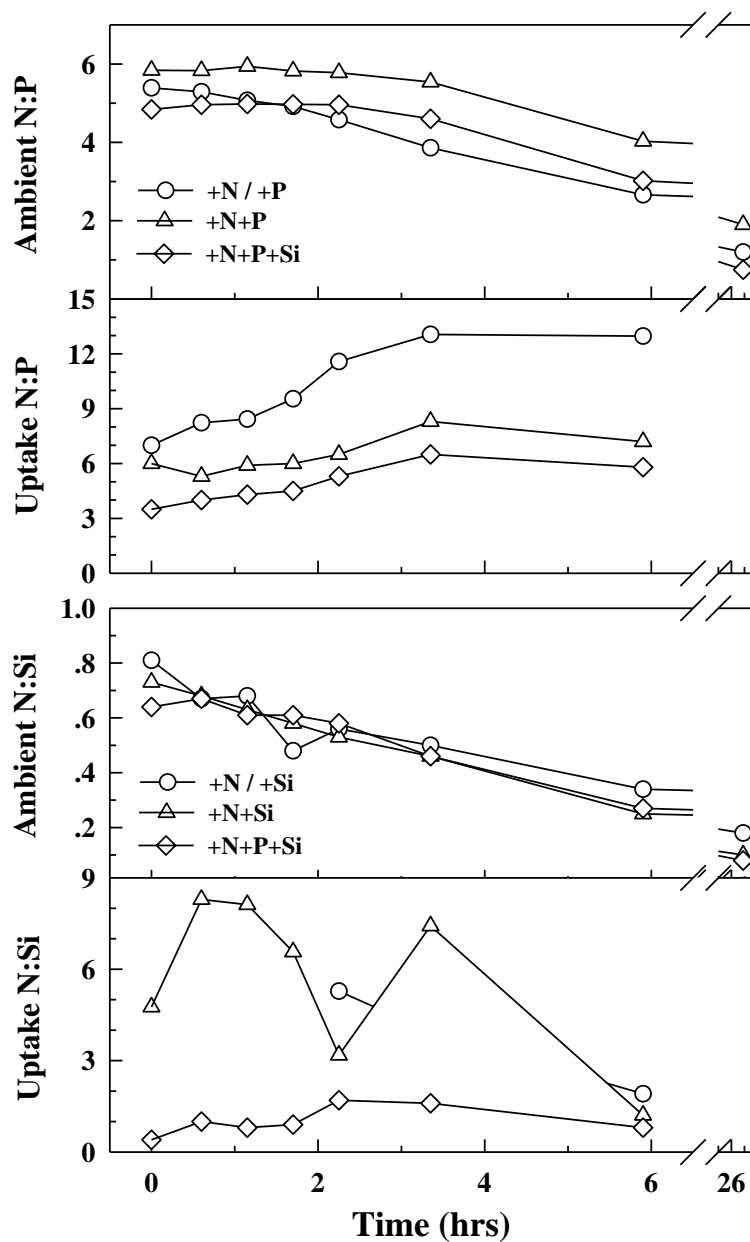


Fig. 10

